Proper Orthogonal Decomposition (POD):

Application to Finite Element Analysis of Electromagnetic Diffusion

By

Farasatul Adnan

Department of Electrical and Computer Engineering

McGill University, Montreal

February, 2011

A thesis submitted to McGill University in partial fulfillment of the requirements of the degree of Master of Engineering

Table of Contents

Acknowledgements

I would like to express my sincere gratitude to my supervisor, Professor Jonathan P. Webb for his guidance and foresight, without which this thesis would not have been possible. It was an honour for me to have had him as my supervisor and the learning experience was a very fulfilling one.

I would like to thank my parents for everything they have taught me. Without their love and support, I would not be here today. I can never repay you in any way but I hope I have been a worthy son.

Finally, I would like to thank my fellow graduate students of the CAD lab for their cooperation and friendship. Special thanks are due for Mr. Rajeev Das and Mr. Jun Ouyang for being there for me whenever things got tough.

Abstract

Proper Orthogonal Decomposition (POD) is a technique which has been used successfully to reduce the computation time in various fields of engineering. Here POD is applied to electromagnetic field computations, specifically to the simulation of electromagnetic diffusion by the time-domain finite element method. The standard method requires a large matrix equation to be solved at every time step. POD is applied to greatly reduce the size of the matrices. Both 1-D and 2-D test cases are considered. Applying POD reduces the matrix dimension for a 2-D problem from 2,535 to just 5, with negligible loss of accuracy.

Résumé

La Décomposition Orthogonale Nécessaire (POD) est une technique qui a été utilisée avec succès pour réduire le temps de compte dans les champs différents d'ingénierie. Ici la POD est appliqué les comptes électromagnétiques de terrain, spécialement à la simulation de la diffusion électromagnétique par le domaine de temps la méthode d'élément finie. La norme la méthode exige à une grande équation matricielle d'être résolue au pas de chaque fois. La POD est appliquée beaucoup réduire la grandeur du matrices. De 1ème que 2ème cas tant d'essai sont considérés. L'application de la POD réduit la dimension matricielle pour un 2ème problème de 2,535 à juste 5, avec la perte négligeable d'exactitude.

1 Introduction

Modern electrical engineering deals with various time consuming computer simulations. One particular field of such computations involves electromagnetic systems. The modern world depends on these to a great extent: radar systems, microwave ovens, mobile telephones, satellite communications, electrical motors, medical imaging systems and transformers, to name a few. Therefore, it is no surprise that the field of electromagnetic simulation continues to grow.

Even with the advent of fast computers, numerical analysts try to use various mathematical tools to reduce computational costs (i.e. computation time). Proper Orthogonal Decomposition (POD) is one such mathematical tool. It was first introduced by Karl Pearson in 1901 [1]. Data analysis using the POD is conducted to extract 'mode shapes' or 'basis' functions, from experimental data of high-dimensional systems, for subsequent use in Galerkin projections that yield low dimensional dynamical models. In this way, we can greatly reduce computational cost.

Nowadays, POD finds applications in many fields of engineering analysis: chemical engineering [2], fluid mechanics [3], image processing [4], aerospace engineering [5], MEMS [6], oceanography [7], structural dynamics [8], etc. However, it has not been used before in electromagnetics (EM).

One important class of EM field problems is the diffusion of EM fields and currents in conductors. It arises, for instance, in the measurement of induction currents in the earth,

which can provide resistivity maps for geophysical prospecting [9] but the main class of applications is in electromechanical devices of various sorts: motors, actuators, etc. The concern of this thesis is in the solution of such problems by time-stepping methods.

There are quite a few numerical methods that have been applied to EM field problems. The finite-difference time-domain (FDTD) method is a popular computational modeling technique. It solves the partial differential equations (PDEs) directly, without using variational principles or weighted residuals. The fields are computed on a regular grid with a marching-on-in-time discretization of time. The term FDTD comes from the update equations where field values at the next time step are found from the field at that moment and the previous time step. Its great appeal is its simplicity and ease of coding. It also does not require any storage of large matrices and thus requires very low disk space. The primary drawback is inflexible meshing and uncertainty about the precise position of boundaries. For oblique boundaries, FDTD programs typically resort to the "staircase approximation". The error due to the staircase approximation can be difficult to assess. Dispersive materials also need some effort to implement [10], [11], [12].

The boundary element method (BEM) is another numerical method for solving linear partial differential equations. It is also referred to as the method of moments (MoM). The BEM discretizes Maxwell's equations in integral form. The unknowns are sources such as currents or charges on material interfaces. This method is advantageous for problems involving open regions. It has been thought preferable to differential-equation formulations because a mesh is only needed for surfaces, not volumes. The key

advantage is a reduction of the number of variables, but the resulting matrices are usually dense and so it rarely saves time or memory [13].

The Finite Element Method (FEM) is a good choice for solving partial differential equations over complicated domains. The FEM can be derived in two different ways: by variational principles, or by the method of weighted residuals. The former involves a functional whose minimum is the solution of a PDE and associated boundary conditions. The latter uses integrals of the weighted error (residual) over the problem domain. Both usually end up with identical equations. The field is discretized using meshes of simple geometric shapes (e.g., triangles, tetrahedra) called "elements". The FEM can handle both eigenanalysis (source free) and deterministic (driven) problems [14].

A drawback of time-domain FEM (TD-FEM) is that it is implicit, i.e., a system of equations needs to be solved at each time step. The systems can be written as a matrix equation in which the matrix is sparse, but typically very large.

The key attraction of time stepping schemes is their simplicity. The simplest is the Euler scheme. In this method, the approximation of an equation of this form

$$\frac{\partial \phi(t)}{\partial t} = F(t)$$

is: $$\frac{\phi(t+\Delta t)-\phi(t)}{\Delta t} = F(t)$$

Here, you can predict the next ϕ value based only on the current fields (where ϕ represents the field) [14].

However, time stepping can be costly, especially when we have to simulate a rapidly changing field for a long time, as can be the case when moving through an initial transient to reach a steady state. The computational cost is directly related to the size of the time step. The smaller the time step the longer it takes for the simulation to get through the transient, but larger time steps lead to lower accuracy.

Some other methods are used as alternatives to time stepping, but they have limitations. Phasor analysis can be used [15], but it is good for linear problems only. Also, phasor analysis only finds the steady state response. For problems where the transient behaviour is of interest, it is not a valid option.

Multi-harmonic method is another option [16], but it is expensive. The number of unknowns increases with the number of harmonics and this leads to high computational costs.

The FEM leads to sparse matrices that are solved most efficiently using iterative techniques. However, when the problems are large and where the matrices have a dimension of 10^6 or more, it is naturally imperative that we search for a method that can reduce the computations involved even further. The objective of this thesis is to solve an EM diffusion problem using TD-FEM accelerated by POD. POD has been used to speed up TD-FEM calculations before (for instance, for problems of thermal analysis [17]), but in EM it is new. There are other methods which are also being used for solving the problem of concern in this thesis. For instance, the singularity decomposition (SDT)-explicit error correction method (EEC) [18]. In this method one constructs a linear system

of auxiliary equations by applying the SDT-based EEC (SD-EEC) method to TP (Time Periodic)-FEM. The correction of the error components obtained by solving the linear system of auxiliary equations efficiently accelerates the convergence of transient calculation.

Here is a brief outline for the thesis. Chapter 2 describes the diffusion problems to be solved and their FEM formulation. Chapter 3 discusses POD and how it works, i.e., the underlying mathematics behind POD and how it can be used for TD-FEM. Chapter 4 presents results for test cases solved with the new method. Chapter 5 draws conclusions and looks at future possibilities for the application of POD in computational EM.

2 FEM Formulations for Magnetic Diffusion

2.1 Problem using 1-D Finite Elements

In this section, the problem of diffusion into a slab of copper is considered. The metal is assumed to have conductivity σ and permeability μ. For simplicity, the slab is assumed to be very broad and long compared to its thickness, so that the field variations need only be considered in the direction across the slab, which is taken to be the *x*-direction. Co-ordinate axes are chosen so that the magnetic field in the metal points in the *y*-direction (Fig. 1). Therefore, the problem is one of solving the 1-D diffusion equation subject to boundary conditions.

The *y*-component of magnetic field in the slab of copper is governed by this equation [19], [20]:

$$\frac{d^2 H_y}{dx^2} = \sigma\mu \frac{dH_y}{dt} \tag{2-1}$$

which is known as the *diffusion equation* because of its similarity to the equation arising in heat diffusion problems. The problem being considered is similar to a heat diffusion problem, only it is magnetic field that is diffusing rather than temperature.

We assume there is a net sinusoidal current $2I_0 \sin(\omega t)$ flowing through the conductor in the *z*-direction and that the full slab thickness is *2L*. We can model one half of the slab (from *x*=0 to *x*=*L*) by applying a symmetry condition of

$$H_y = 0 \qquad \text{at } x=0$$

At the other end $x=L$ (Fig. 1) the boundary condition for H_y is found using Ampere's Law:

$$\oint H_y.dl = I$$

Applying this to the rectangular perimeter in Fig. 1 gives

$$H_y = I_0 \sin(\omega t) \quad \text{A/m}$$

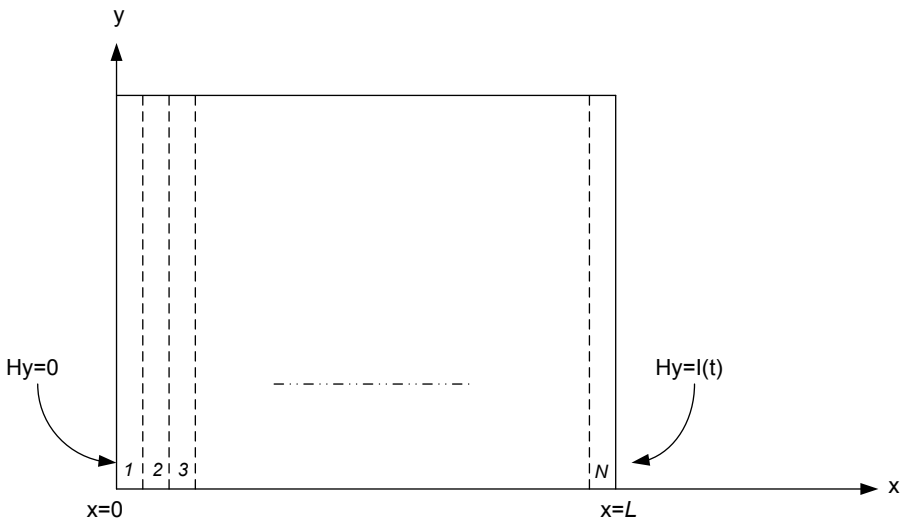

Fig. 1

One half of the copper slab of thickness $2L$ for 1-D finite element analysis.

Equation (2-1), together with these boundary conditions, can then be solved using Galerkin's method or the Ritz variational method [14].

Applying Galerkin's method, the residual for a given approximate solution H_y is

$$\frac{d^2 H_y}{dx^2} - \sigma\mu \frac{dH_y}{dt} = r \qquad (2\text{-}2)$$

Discretizing the problem region into N finite elements (Fig. 1), the weighted residual integral for the e-th element can be written as

$$R_i^e = \int_{x_1^e}^{x_2^e} N_i^e r \, dx \quad i=1, 2. \tag{2-3}$$

Here the weight function is N_i^e and is the first order interpolation function given by

$$N_1^e = \frac{x_2^e - x}{l^e} \quad \text{and} \quad N_2^e = \frac{x - x_1^e}{l^e}$$

where l^e is the size of a single 1-D finite element.

Substituting (2-2) into (2-3) and integrating by parts for the first term on the right hand side yields

$$R_i^e = \int_{x_1^e}^{x_2^e} \left[\frac{dN_i}{dx} \frac{dH_y}{dx} - \sigma\mu N_i \frac{dH_y}{dt} \right] dx \tag{2-4}$$

Now, we use this interpolation for H_y in element e:

$$H_y^e = \sum_{j=1}^{2} N_j^e(x) \; H_{y_j}^e \tag{2-5}$$

Substitution of (2-5) in (2-4) for H_y leads to the elemental residuals

$$R_i^e = \sum_{j=1}^{2} H_{y_j}^e \int_{x_1^e}^{x_2^e} \left[\frac{dN_i}{dx} \frac{dN_j}{dx} - \sigma\mu N_i \frac{dN_j}{dt} \right] dx \tag{2-6}$$

or in matrix form

$$\left\{R^e\right\} = [S]\left\{H_y^e\right\} - [T]\frac{d}{dt}\left\{H_y^e\right\} \tag{2-7}$$

where

$$S_{ij}^{e} = \int_{x_1^e}^{x_2^e} \left(\frac{dN_i^e}{dx} \frac{dN_j^e}{dx} \right) dx \qquad i=1, 2 \qquad (2\text{-}8)$$

&

$$T_{ij}^{e} = \sigma\mu \int_{x_1^e}^{x_2^e} \left(N_i^e N_j^e \right) dx \qquad i=1, 2 \qquad (2\text{-}9)$$

$\left[S\right]^e$ and $\left[T\right]^e$ for a single element can be evaluated explicitly:

$$\left[S\right]^e = \begin{bmatrix} \frac{1}{l} & \frac{-1}{l} \\ \frac{-1}{l} & \frac{1}{l} \end{bmatrix} \quad \text{and} \quad \left[T\right]^e = \begin{bmatrix} \frac{l}{3} & \frac{l}{6} \\ \frac{l}{6} & \frac{l}{3} \end{bmatrix} \qquad (2\text{-}10)$$

The overall residual is obtained from the elemental residuals, after going through the FE standard assembly process:

$$\left[S\right]\left\{H_y\right\} - \left[T\right]\frac{d}{dt}\left\{H_y\right\} = 0 \qquad (2\text{-}11)$$

Now, since there are N elements, we will have (N+1) nodes and therefore the matrices in (2-11) have dimension (N+1). The (N+1)-st node and the 1st node are nodes with a *prescribed* value but the rest of the nodes are *free*.

Rewriting the system of equations for $\left[S\right]$ and $\left[T\right]$ in terms of the free and the prescribed nodes, one can rewrite $\left[S\right]$ as

$$\begin{bmatrix} S_{ff} & S_{fp} \\ S_{pf} & S_{pp} \end{bmatrix}$$

and $[T]$ as

$$\begin{bmatrix} T_{ff} & T_{fp} \\ T_{pf} & T_{pp} \end{bmatrix}$$

The subscript *p* corresponds to nodes that are prescribed, and which should therefore not have had any weight functions associated with them in (2-3). Therefore, they must be dropped at this point. In addition, node 1 is prescribed to the value 0. Then (2-11) becomes

$$[S_{ff}]\{H_y\} + [S_{fp}]\{H_{y\ N+1}\} - \sigma\mu[T_{ff}]\frac{d}{dt}\{H_y\} - \sigma\mu[T_{fp}]\frac{d}{dt}\{H_{y\ N+1}\} = 0 \qquad (2\text{-}12)$$

The value for $H_{y\ N+1}$ is already known as $I_0\sin(\omega t)$ and it is incorporated in a forcing function f to give

$$[S]\{H_y\} - [T]\frac{d}{dt}\{H_y\} = \{f\} \qquad (2\text{-}13)$$

where $$\{f\} = -[S_{fp}]I_0\sin(\omega t) - \sigma\mu[T_{fp}]\frac{d}{dt}I_0\sin(\omega t) \qquad (2\text{-}14)$$

and $[S] = [S_{ff}]$ and $[T] = [T_{ff}]$ are (*N*-1)x(*N*-1) matrices.

Thus, the formulation for the 1-D FEM problem is complete.

2.2 Problem using 2-D Finite Elements

Next, we consider a 2-D case (Fig. 2). The same mathematical approach applied to the 2-D problem yields a similar equation [13], [14].

For this problem, we consider a copper slab next to a pair of round conducting wires which are carrying current perpendicular to the page (i.e., in the *z*-direction). The slab has length 10 cm but the problem is symmetrical so we only analyze the right hand half of the problem region. We assume that the geometry shown in Fig. 2 is infinite in the z-direction and that the fields do not vary in this direction. It is then possible to show that the magnetic vector potential **A** has only one component A_z, also known as the flux function. This will simply be referred to as A in the following.

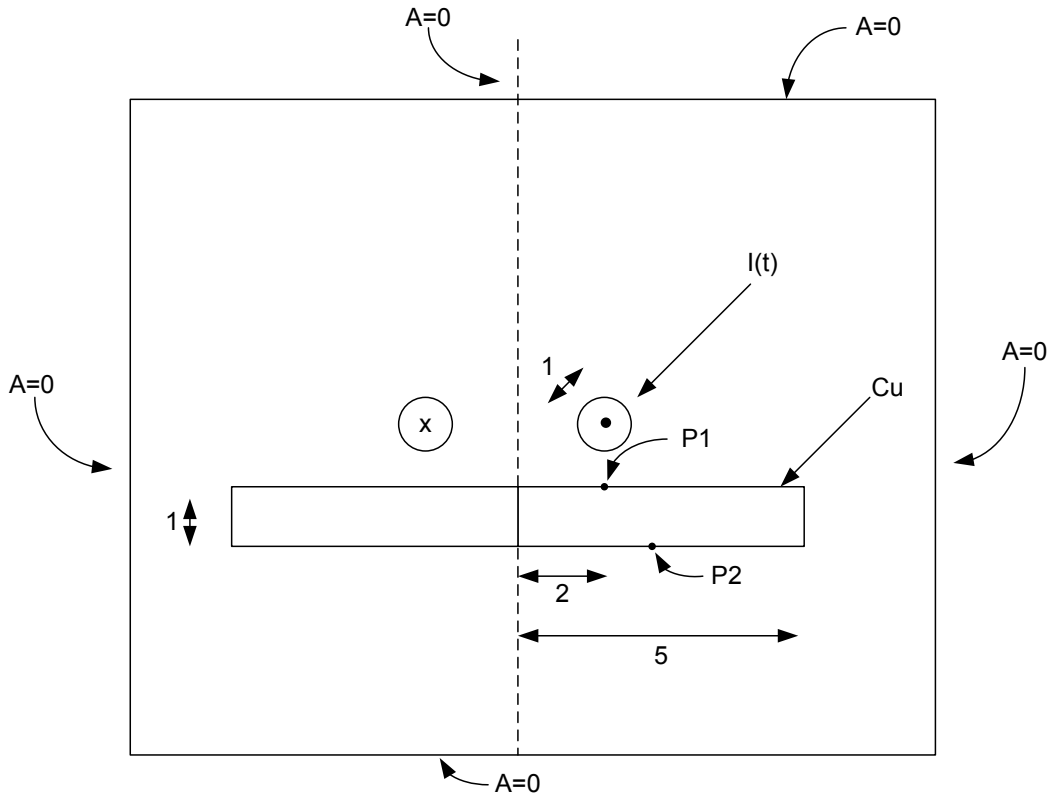

Fig. 2

A copper slab for 2-D finite element analysis with appropriate boundary conditions. The circular shape on the right represents a wire carrying current in the +*z* direction. The corresponding shape on the left is a wire carrying the same current in the –z direction. Dimensions are in cm. $I(t)= I_0 \sin(\omega t)$.

A mesh of triangular finite elements for this geometry was created using commercial software [21]. The mesh is shown in Fig. 3. Application of Galerkin's method leads to an equation similar to (2-13) except that now $\{f\} = \{f_0\} * I_0 \sin(\omega t)$, where $\{f_0\}$ is time-independent. The $[S]$, $[T]$ and $\{f_0\}$ matrices were created for this geometry using the same commerical software [21].

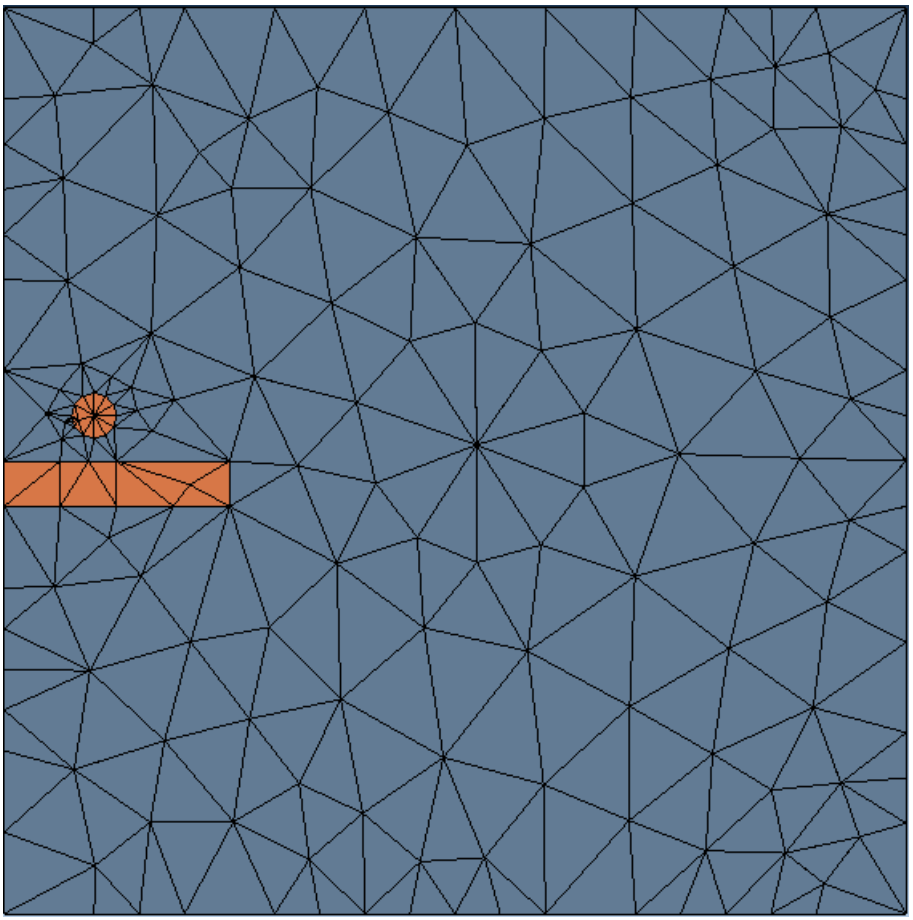

Fig. 3

The FE mesh for the problem shown in Fig. 2 [21].

2.3 Time-Domain FEM and Time Stepping Schemes

As we see, when TD-FEM is used to solve magnetic diffusion problems, we arrive at a

matrix equation of this form:

$$[S]\{u(t)\} + [T]\frac{d}{dt}\{u(t)\} = \{f(t)\} \tag{2-15}$$

which is an equation where $[S]$ and $[T]$ are square matrices and $\{u(t)\}$ is the vector of unknowns. $\{f(t)\}$ is the right-hand side vector which contains the forcing function. In general, the matrix $[S]$ depends on $\{u(t)\}$ because of the non-linear properties of the magnetic materials, but in this work we assume that the materials are linear, so the system (2-15) is linear in {u(t)}.

Here, $\{u(t)\}$ is an *m*-vector which stores the time-varying field or potential. For this thesis, the entries of $\{u(t)\}$ are the values of the magnetic field (1-D case) or magnetic vector potential (2-D case) at nodes of the finite elements.

There are various time-stepping schemes that can approximately solve equation (2-15). These essentially employ a finite difference scheme to discretize in the time domain. For this, we first divide the time axis uniformly into a number of time intervals. Each interval is referred to as a time step. In this thesis, backward Euler time-stepping scheme is used, but we briefly review a number of methods.

A function of $u(t+\Delta t)$ can be expanded to a Taylor series about *t* as

$$u(t+\Delta t) = u(t) + \frac{du}{dt}\Delta t + \frac{d^2u}{dt^2}(\Delta t)^2 \,{}^{1}\!/_{2!} + O[(\Delta t)^3]$$

where the last term represents the sum of the remaining terms. Truncating this series we obtain approximately

$$\left.\frac{d}{dt}\{u(t)\}\right|_k \approx \frac{\{u_{k+1}\}-\{u_k\}}{\Delta t} \tag{2-16}$$

where *k* refers to the fact that it is evaluated at the end of time step *k* and Δt is the duration of the time step. If (2-16) is substituted in (2-15), we can evaluate $\{u(t)\}$ at a time instant (*k*+1) if we know $\{u(t)\}$ at time instant *k*. This is also referred to as the forward Euler or the forward difference method [14].

Similar to the forward difference method is the backward difference method. For a given function $u(t-\Delta t)$, the Taylor series expansion is

$$u(t-\Delta t) = u(t) - \frac{du}{dt}\Delta t + \frac{d^2u}{dt^2}(\Delta t)^2\ {}^{1}\!/_{2!} + O[(\Delta t)^3]$$

which again can be approximated as

$$\left.\frac{d}{dt}\{u(t)\}\right|_k \approx \frac{\{u_k\}-\{u_{k-1}\}}{\Delta t}$$

and then (2-15) can be solved similarly [14].

Now, if we subtract $u(t-\Delta t)$ from $u(t+\Delta t)$ we get

$$\frac{d}{dt}\{u(t)\} \approx \frac{u(t+\Delta t)-u(t-\Delta t)}{2\Delta t}$$

which is the central difference approximation. For discretized time this leads to

$$\frac{d}{dt}\{u(t)\}\Big|_k \approx \frac{u_{k+1}-u_{k-1}}{2\Delta t}$$

Again, if we have the value for u_{k-1} we can obtain the value of u_{k+1} using (2-15) [14].

Another useful method is the Newmark-Beta method. In this method we write $u(t+\Delta t)$ as

$$u(t+\Delta t) = u(t) + \frac{du}{dt}\Delta t + \frac{d^2u}{dt^2}(\Delta t)^2(\frac{1}{2}-\beta) + \beta(\Delta t)^2\frac{d^2u(t+\Delta t)}{dt^2}$$

where β is a parameter that can be chosen to control the accuracy of the time marching process [14].

Now, applying the backward Euler scheme and using equation (2-16), we can write equation (2-15):

$$[S]\{u_k\}+[T]\left(\frac{\{u_k\}-\{u_{k-1}\}}{\Delta t}\right) = \{f_k\}$$

This can be rearranged to give us a matrix problem for $\{u\}$ at time k in terms of an earlier $\{u\}$ at time (k-1) as

$$\left([S] + \frac{1}{\Delta t}[T]\right)\{u_k\} = \{f_k\} + \frac{1}{\Delta t}[T]\{u_{k-1}\} \qquad (2\text{-}17)$$

Thus, we have an equation for discrete time samples which needs to be solved iteratively.

3 POD Formulation

3.1 Brief history and outline of POD

The problem of finding the closest fitting lines or planes to a set of points in space was investigated by Pearson [1] using the earliest formulation of POD. Independently, almost three decades later, a similar treatment appeared by Hotelling [22] where the term "method of principal components" was coined. POD seems to have been re-invented quite a few times by different people over the last century. Among them are Karhunen [23] and Loeve [24]. According to its field of application, POD has also been dubbed the Karhunen-Loeve Transform (KLT), the Hotelling Transform, Principal Component Analysis (PCA) and Singular Value Decomposition (SVD).

In the following, the main ideas of POD are discussed.

Let us assume that one measurement of some system is represented by a column vector of *m* real numbers. If we have *n* such measurements, the whole set of measurements can be represented by an *m*x*n* matrix $[U]$. Suppose the measurements are quite similar, in which case the columns of $[U]$ are almost linearly dependent. It is often of interest to approximate the *n* vectors in $[U]$ by a smaller number *l,* of *orthogonal* vectors that can represent all the mesaurements in $[U]$ reasonably accurately. Let this smaller set be the columns of the *m*x*l* matrix $[V]$. POD provides us with a way of calculating a $[V]$ that is

guaranteed to be the "best" approximation of $[U]$ that can be achieved using only l vectors, in the sense that the distance between $[V]$ and $[U]$ is minimized.

If $n<<m$, the most efficient procedure is to solve this nxn symmetric eigenproblem for the l largest eigenvalues:

$$[U]^T [U]\{x\} = \lambda \{x\} \tag{3-1}$$

Suppose the eigenvalues are $\lambda_1 \geq \lambda_2 \geq \lambda_3 \geq ..... \geq \lambda_l > 0$.

The columns of $[V]$ are then given by

$$\{v^i\} = \frac{1}{\sqrt{\lambda_i}}[U]\{x^i\} \qquad i=1, 2, 3……..l \tag{3-2}$$

This theory is applied in the next section to the TD-FEM problem.

3.2 Applying the snapshot method to obtain a new basis

The problem we have to solve in TD-FEM is given by (2-18), repeated here for convenience:

$$\left([S] + \frac{1}{\Delta t}[T]\right)\{u_k\} = \{f_k\} + \frac{1}{\Delta t}[T]\{u_{k-1}\} \tag{3-3}$$

This equation is used to obtain $\{u\}$ at instant k from $\{u\}$ at instant (k-1), and in this way we march forward in time. When we have marched forward by (n-1) steps ($n<<m$), we

will have *n* 'snapshots' [25] of $\{u\}$ at times Δt , $2\Delta t$, $3\Delta t$ … $(n-1)\Delta t$.

Now, if *n* is a large enough number, we might think of these first *n* solutions as a new basis for $\{u\}$. We can write

$$\{u(t)\} = [U]\{c(t)\} \tag{3-4}$$

where $[U]$ is an *m*x*n* matrix whose columns are the *n* snapshots and $\{c(t)\}$ is now a much shorter vector of coefficients. $[U]$ is a fixed matrix that does not vary in time. Applying (3-4) at a time instant *k* we get

$$\{u_k\} = [U]\{c_k\}$$

If we substitute this into (3-3), we get

$$\left([S] + \frac{1}{\Delta t}[T]\right)[U]\{c_k\} = \{f_k\} + \frac{1}{\Delta t}[T][U]\{c_{k-1}\}$$

Now we make these matrices smaller by pre-multiplying by $[U]^T$

$$[U]^T\left([S] + \frac{1}{\Delta t}[T]\right)[U]\{c_k\} = [U]^T\{f_k\} + \frac{1}{\Delta t}[U]^T[T][U]\{c_{k-1}\}$$

$$\text{or,} \quad \left([S'] + \frac{1}{\Delta t}[T']\right)\{c_k\} = \{f'_k\} + \frac{1}{\Delta t}[T']\{c_{k-1}\} \tag{3-5}$$

where

$$[S'] = [U]^T [S][U]$$
$$[T'] = [U]^T [T][U]$$
$$\{f'_k\} = [U]^T \{f_k\}$$

Now the matrices $[S']$ and $[T']$ are nxn instead of mxm. We have reduced the size of the matrices and can continue to step forward in time much more efficiently.

There is a problem in this process. In general, there is near linear dependence amongst the n snapshots and so, the new matrices tend to be very ill-conditioned.

3.3 Applying POD to the TD-FEM Problem

POD gives us a way of finding a smaller set of l fully independent (in fact, mutually orthogonal) vectors $\{v^i\}$, which is the best approximation to our n snapshots.

To do this, as described in section 3.1, we find the l largest eigenvalues and corresponding eigenvectors of the equation

$$[U]^T [U]\{x\} = \lambda\{x\} \tag{3-6}$$

where $\{x\}$ is the eigenvector and λ is the eigenvalue. Here, the eigenvectors will be of length n because $[U]^T[U]$ is of size nxn. These eigenvalues and eigenvectors are calculated using Matlab's built-in function 'eig' [26], which computes all the eigenvalues of a square symmetric matrix by first reducing the matrix to tri-diagonal form, then

applying the QR algorithm [27].

$[U]^T[U]$ is a dense matrix, but finding the eigenvalues and corresponding eigenvectors is computationally inexpensive because *n* is a relatively small number. As will be shown in the coming chapter, we can get satisfactory results using an *n* in the range 10 to 20.

Once we have these values, we can calculate

$$\{v^i\} = \frac{1}{\sqrt{\lambda_i}}[U]\{x^i\} \qquad i=1, 2, 3\ldots l \tag{3-7}$$

Knowing these *l* vectors, we can replace (3-4) by

$$\{u(t)\} = [V]\{c(t)\} \tag{3-4'}$$

where $[V]$ is an *m*x*l* matrix whose columns are the vectors $\{v^i\}$. Following the same path as described before, we will end up with (3-3) again, but this time we will have matrices which are *l*x*l* in size and are well-conditioned. The problem of ill-conditioned matrices is solved because the vectors $\{v^i\}$ are mutually orthogonal.

Thus POD helps us get computational results much more quickly and efficiently.

4 Results from simulations using Standard Time Stepping

The main focus of this thesis work is to solve problems of EM diffusion using both standard time stepping and POD and then to compare the results, with a special interest in the transient phase of the diffusion. The simulations were carried out using MATLAB version R2009b running on a DELL Inspiron 1545 with an Intel Pentium Core 2 Duo processor 2.10 GHz, RAM of 4.00 GB and Windows Vista operating system (64 bit).

4.1 Results for 1-D Problem with Simplified Boundary Conditions

For the 1-D problem (2.2), at first a simplified boundary condition is considered.

Referring to Fig. 1, at $x=L$ a boundary condition of $H_y = 1$ is applied while at $x=0$ the boundary condition remains as shown. Therefore, the problem became similar to the thermal problem of raising one end of a bar initially at 0^0C to 1^0C and holding it at that temperature. One can expect the temperature to decay exponentially along the bar and we have to move through a transient to reach a steady state. The same can be expected for the magnetic field intensity in the material.

From equation (2-14) the forcing function $\{f\}$ now becomes

$$\{f\} = -[S_{fp}] \tag{4-3}$$

We take L=1 m and first look at only 10 elements each with a size of 0.1 m. The matrices are of size 9x9. The simulation is run with a time step of 0.1 s and for 2 iterations.

$\sigma\mu L^2$ has a unit of seconds and represents the time constant of the system. Therefore, for a $\sigma\mu$ of 10 s/m^2, a time step of 0.1 s is sufficient to model the diffusion process accurately in time.

The purpose of such a small number of iterations is to see the transient in its early stages (Fig. 4). In the next simulation we go to 100 iterations (i.e. 10 s) and the resulting curve as expected becomes a straight line (Fig. 5), which is the steady state.

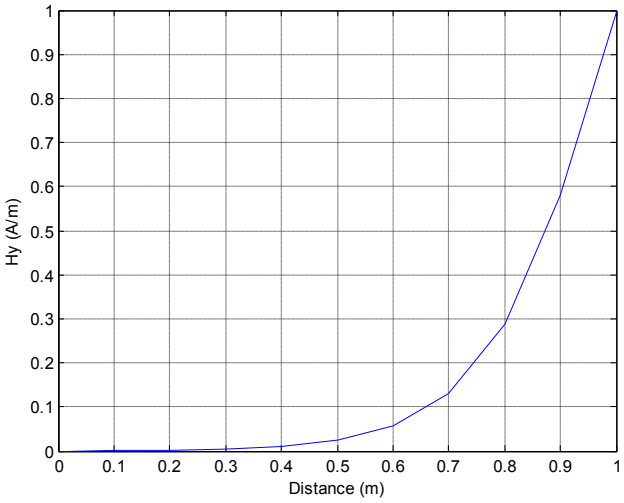

Fig. 4
Simulation involving 10 elements and a boundary condition of Hy=1. Field versus distance after 2 iterations (0.2 s).

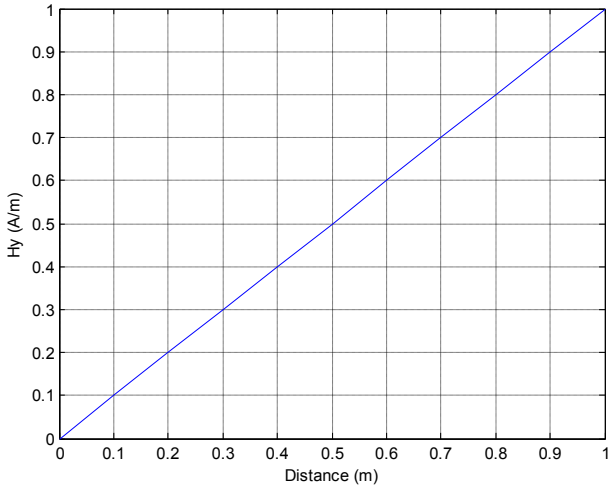

Fig. 5
Simulation involving 10 elements and a boundary condition of Hy=1. Field versus distance after 100 iterations (10 s).

4.2 Results for 1-D Problem with Sinusoidal Boundary Condition

Assuming $I_o = 1$, from (2-14) we get:

$$\{f\} = -[S_{fp}]\sin(\omega t) - \sigma\mu\omega[T_{fp}]\cos(\omega t) \qquad (4\text{-}4)$$

L and $\sigma\mu$ are the same as before. The frequency is 1 Hz and time step is .01 s, i.e., one hundred time steps per period. The skin depth at this frequency is $\delta = \sqrt{\frac{2}{\omega\mu\sigma}}$ =0.178 m.

Now we reduce the size of the elements to 0.01 m, i.e. about 18 elements per skin depth. This gives us matrices with a dimension of *99*x*99* which will give us better accuracy for the calculation of the field on the entire domain. We run simulations for various times (Fig. 6a-Fig. 6e).

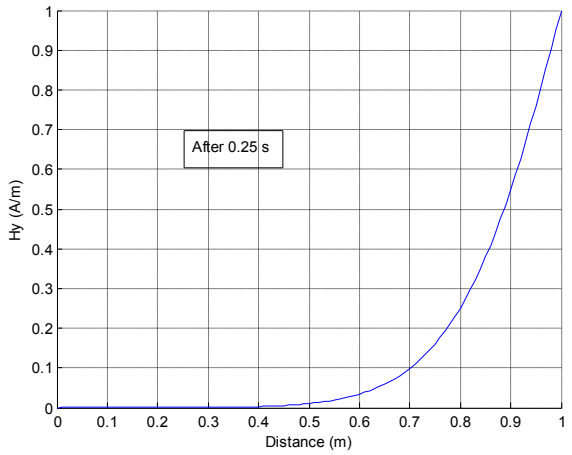

Fig. 6a
Simulations involving 100 elements and a sinusoidal boundary condition at $x=L$ after 0.25 s. Field versus distance.

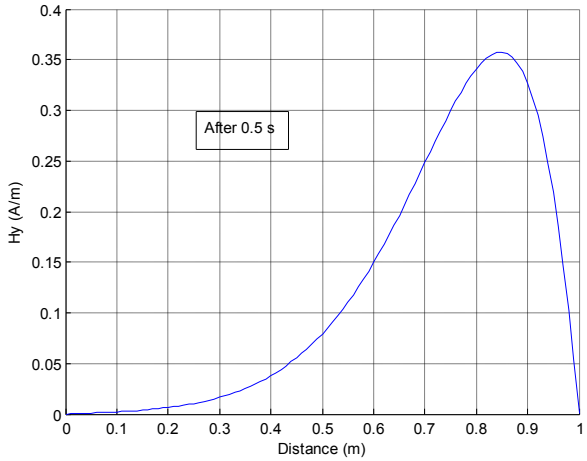

Fig. 6b
Simulations involving 100 elements and a sinusoidal boundary condition at $x=L$ after 0.5 s. Field versus distance.

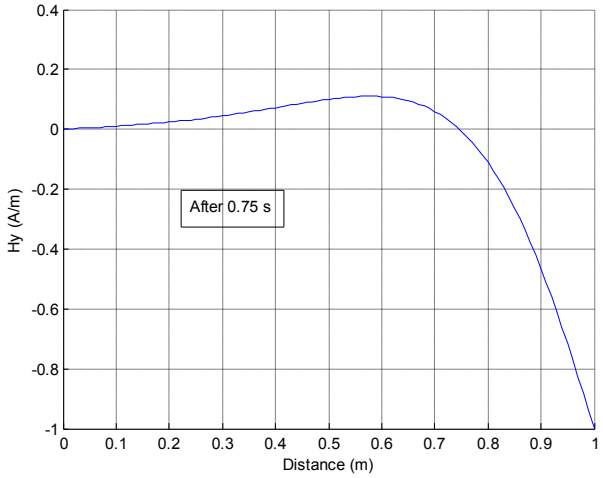

Fig. 6c
Simulations involving 100 elements and a sinusoidal boundary condition at $x=L$ after 0.75 s. Field versus distance.

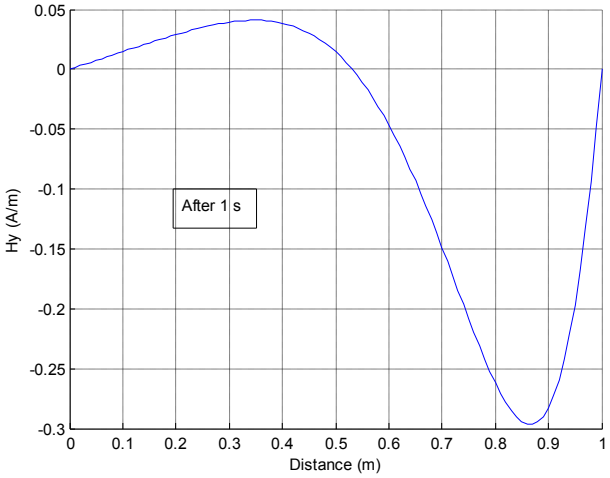

Fig. 6d
Simulations involving 100 elements and a sinusoidal boundary condition at $x=L$ after 1 s. Field versus distance.

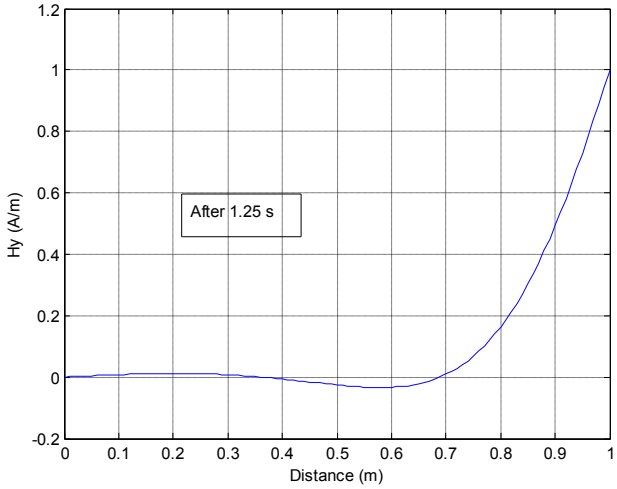

Fig. 6e
Simulations involving 100 elements and a sinusoidal boundary condition at $x=L$ after 1.25 s. Field versus distance.

Now, if we look at the magnetic field at a single node (at x=0.9 m), we see how the field is evolving with time (Fig. 7).

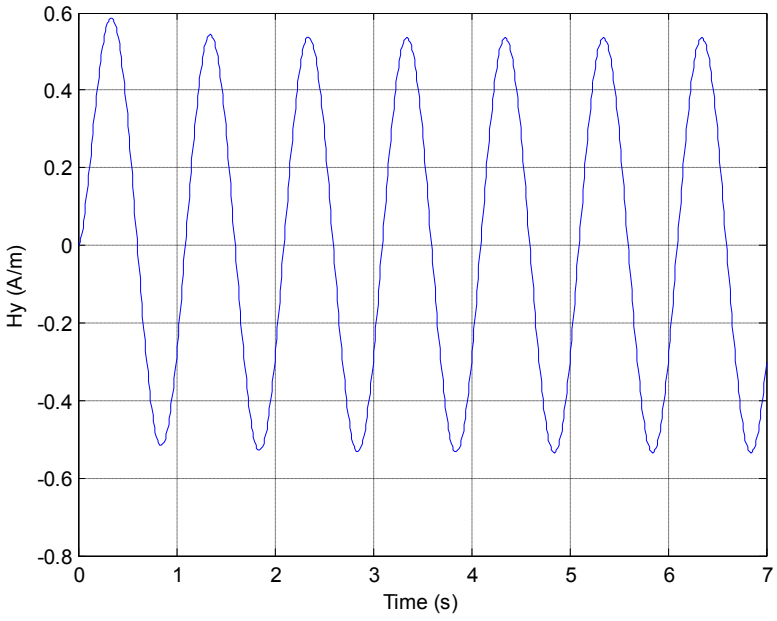

Fig. 7
Magnetic field at x=0.9 m as a function of time

Here we can see that initially the field goes through a slight transient before reaching a steady state.

4.3 Results for 2-D Problem

Standard time-stepping is used to solve the 2-D problem described in section 2.2. The results are compared to those obtained by commercial software [21] using the same mesh (Fig. 3). Figs. 8 and 9 shows the plots obtained when the elements are order 1 (m=183) while Figs. 10 & 11 shows the plots obtained when the elements are order 4 (m=2535). The values of frequency, time step and $\sigma\mu$ were 500 Hz, 0.001 s and 72 s/m^2 respectively.

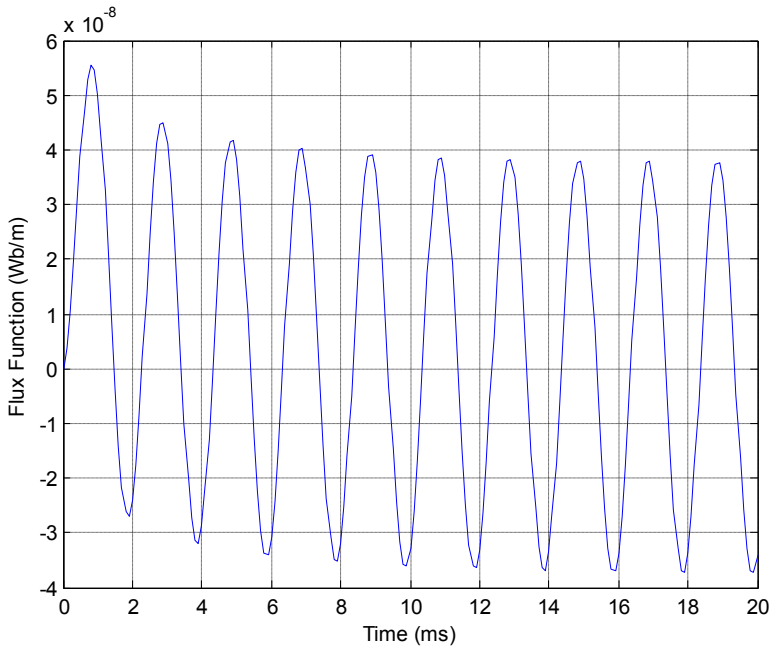

Fig. 8

The flux function, A, at (x,y)=(1.875e-02, 0) m (i.e. P1 in Fig. 2) as a function of time

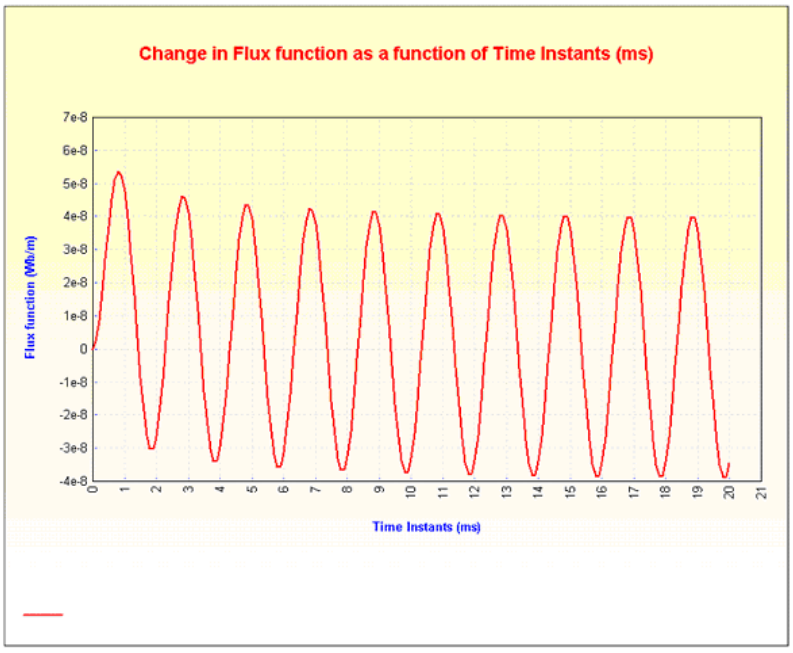

Fig. 9

The flux function, A, at (x,y)= (1.875e-02, 0) m as a function of time, generated by commercial software

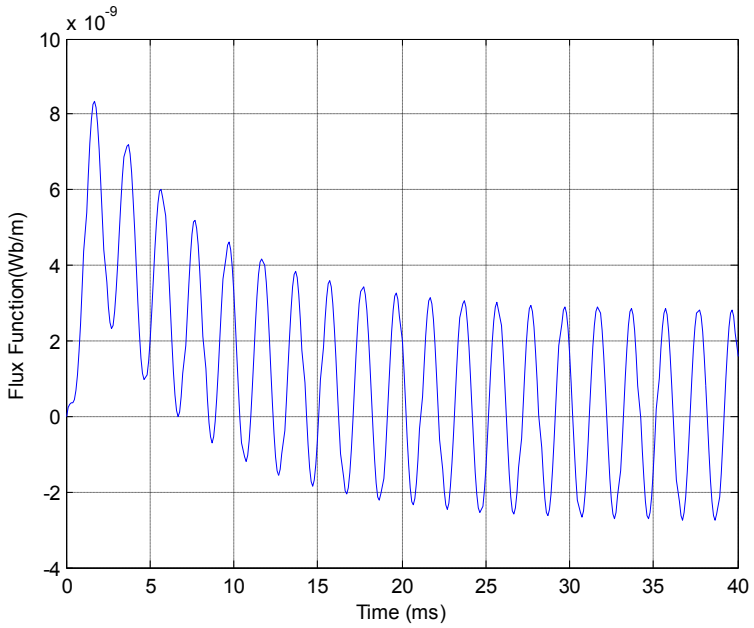

Fig. 10

The flux function, A, at (x,y)=(2.5e-02, -1e-02) m. (P2 in Fig 2) as a function of time

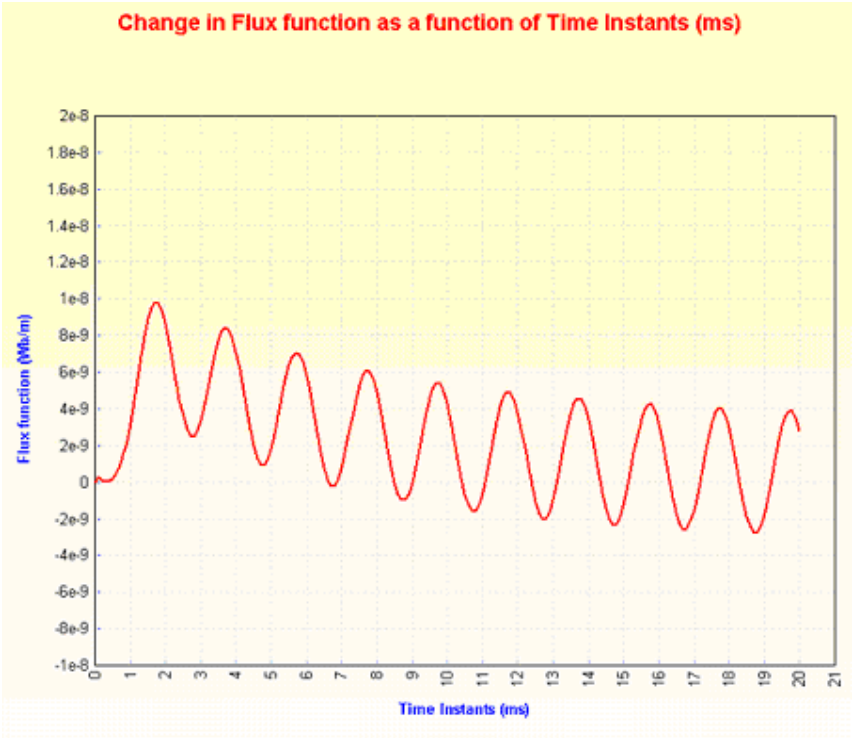

Fig 11

The flux function, A, at (x,y)=(2.5e-02, -1e-02) m, as a function of time, generated by commercial software

4.4 Results using POD: 1D Problem with Sinusoidal Boundary Condition

POD is applied to the 1D problem, with parameters which are the same as in section 4.2. Snapshots are accumulated for the first 0.1 s, i.e., n=10. All 10 corresponding eigenvalues are used (i.e., l=10). The result after 5 s, which is 5 cycles, is shown in Fig. 12.

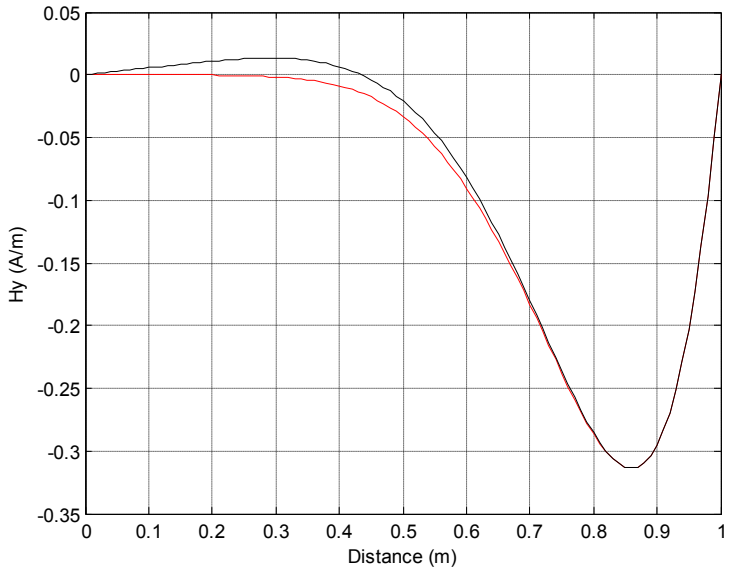

Fig. 12
The magnetic field after 5 s. The curve in red is obtained by POD using n=10, l=10.

Using these parameters the simulation is run to see the time varying fields for the node at x=0.9 m (Fig. 13).

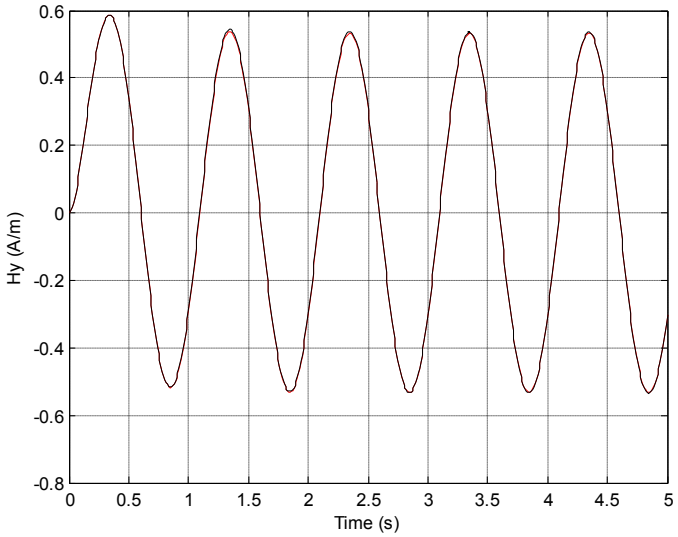

Fig. 13

Magnetic field of the node at x=0.9 versus time. The curve in red is obtained by POD using n=10, l=10.

As we can see the result using POD is extremely accurate (the error is less than 1.2% of the peak value in H_y). Now when we use a smaller basis for instance n=l=5 we get the results in Fig. 14.

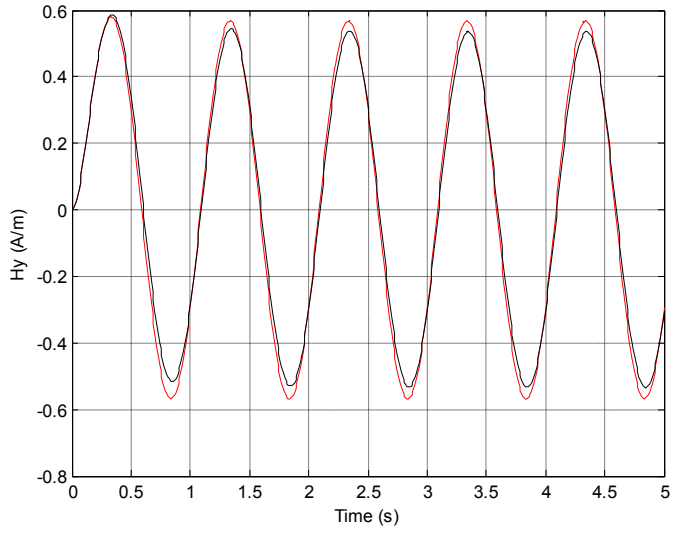

Fig. 14

Magnetic field of the node at x=0.9 m versus time. The curve in red is obtained by POD using n=l=5.

As expected, the smaller basis is giving us a less accurate curve (the error is less than 11% of the peak value in H_y).

Another interesting test is to use a lower number of eigenvalues. Putting n=10 but using only the 3 largest eigenvalues (i.e. l=3) we can get a curve which has a shape fairly close to the one using l=10 (the error is less than 14% of the peak value in H_y). This is beneficial because now the matrices in question will only have a dimension of 3 (Fig. 15).

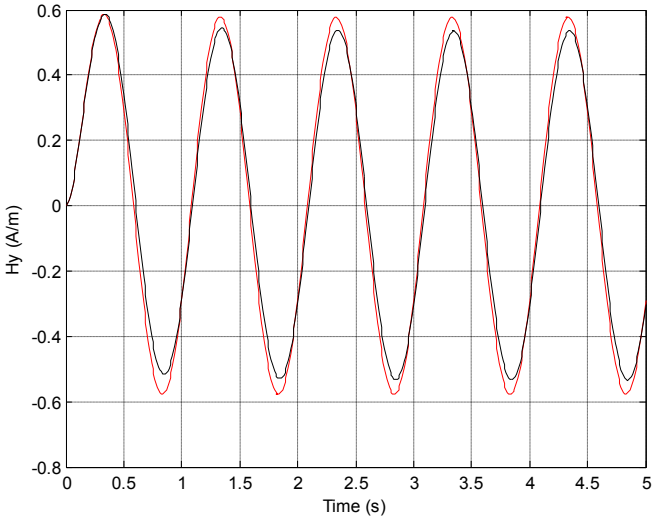

Fig. 15

Magnetic field of the node at x=0.9 m versus time. The curve in red is obtained by POD using n=10, l=3.

When we use higher number of eigenvalues, for example the 5 largest eigenvalues (i.e. l=5), we get a better curve (Fig. 16). Here, the error is less than 5% of the peak value in H_y.

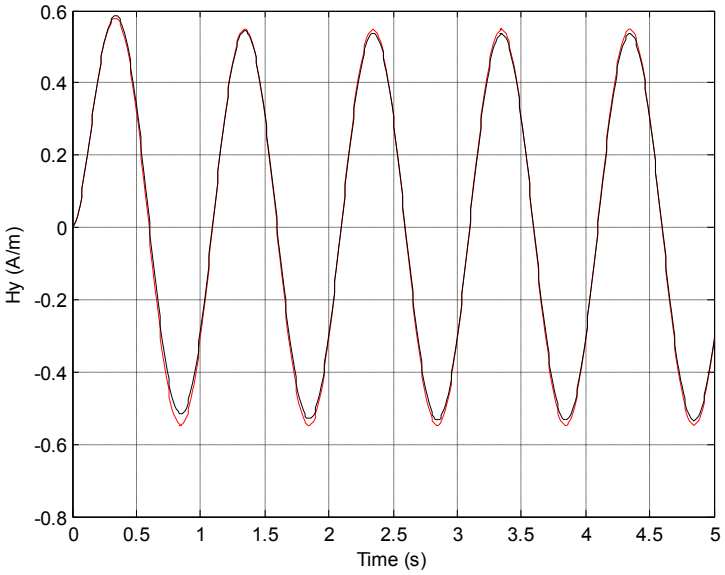

Fig. 16

Magnetic field of the node at x=0.9 m versus time. The curve in red is obtained by POD using n=10, l=5.

4.5 Results using POD: 2D Problem

We use fourth order elements (matrix dimension m=2535) to test POD rather than first order, because we have already seen satisfactory results for smaller matrices from the 1-D test. Here the flux function at P2 (Fig. 2) as a function of time is plotted in Fig. 17.

The parameters are the same as in 4.3. Now n=20 (because it covers one full cycle) and l=4 for the POD curve. A smaller number of eigenvalues are used because the result from the 1-D problem already showed very accurate results when we used all relevant eigenvalues.

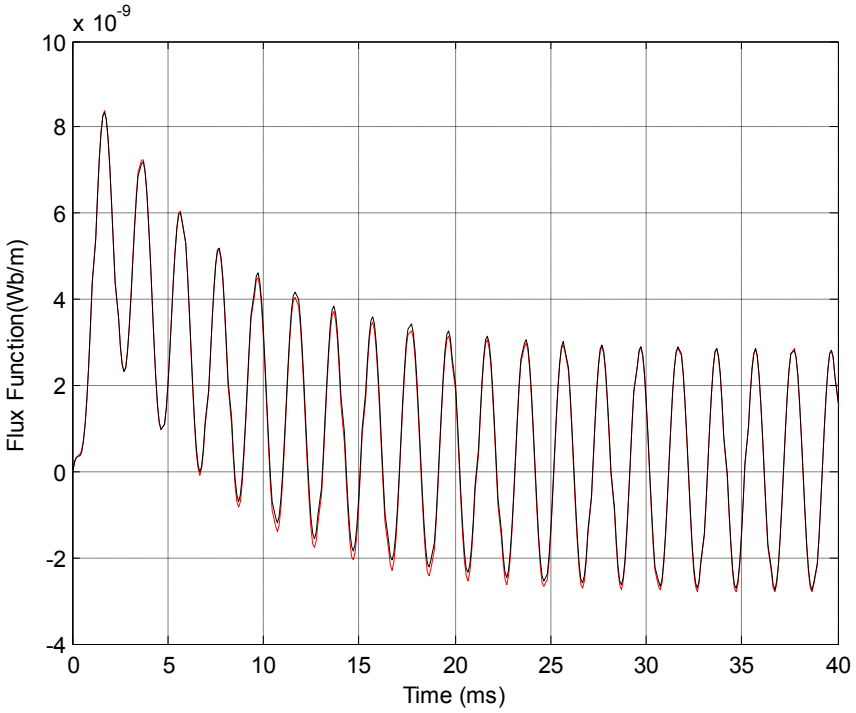

Fig. 17

The flux function at (x, y) = (2.5e-02, -1e-02) for the 2-D structure. The curve in red is obtained by POD using n=20, l=4.

The POD curve (in red) is very accurate (the error is less than 2.7% of the peak value in the flux function). This means a very low computational cost because now the matrices are only of size *4*x*4*.

If we use only the 3 largest eigenvalues we get much more error (Fig. 18). Here, the error is less than 20% of the peak value in the flux function.

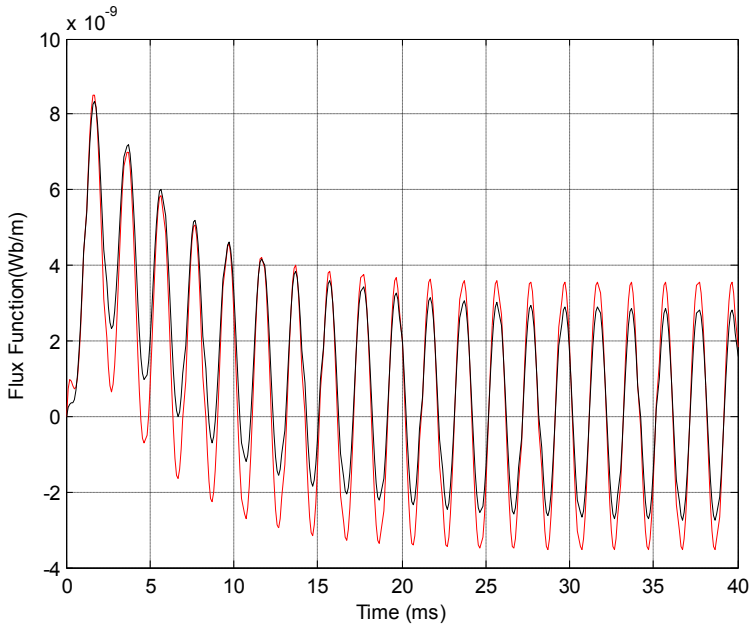

Fig. 18

The flux function at (x, y) = (2.5e-02, -1e-02) for the 2-D structure. The curve in red is obtained by POD using n=20, l=3.

Fig. 19 shows the results when the 5 largest eigenvalues are used. The error is less than 2.4% of the peak value in the flux function.

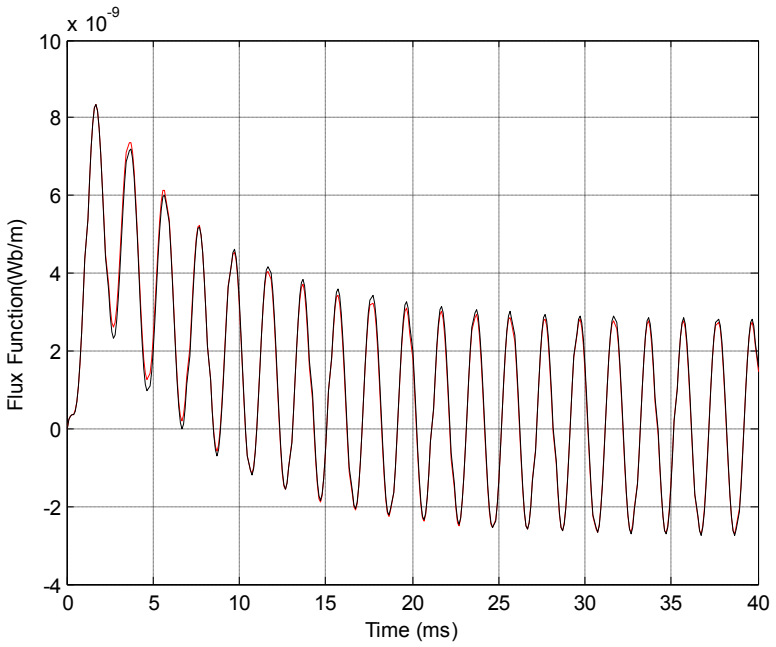

Fig 19

The flux function at (x, y) = (2.5e-02, -1e-02) for the 2-D structure. The curve in red is obtained by POD using n=20, l=5.

If we use even more eigenvalues, we get curves which are indistinguishable from the original. However using all 20 eigenvalues (or a number close to it) creates matrices which are close to singular, but the results remain extremely accurate (Fig. 20). The reason is that when we use a larger number of eigenvalues, some of the basis vectors corresponding to the smaller eigenvalues are nearly linearly dependent on the others. The error is less than 0.004% of the peak value in the flux function.

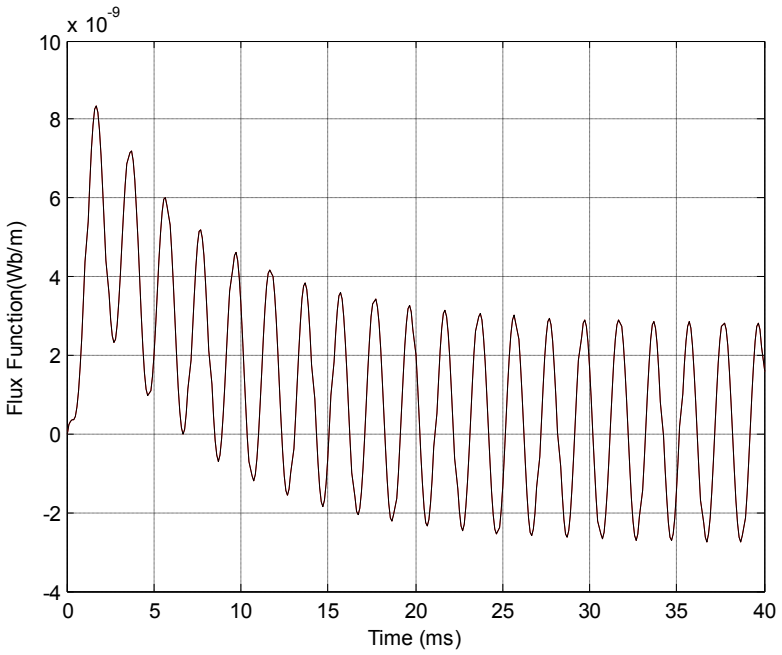

Fig 20

The flux function at (x, y) = (2.5e-02, -1e-02) for the 2-D structure. The curve in red is obtained by POD using n=20, l=20. But the POD curve is not visible because it is overlapping with the original one.

As we are getting accurate results for POD compared to the original time stepping scheme, we can conclude that the code written is working properly. Furthermore, it has been shown that POD is an efficient tool to solve the equations because it uses much smaller matrices. Thus the objective of the thesis is fulfilled.

5 Conclusions

In this thesis, POD has been proposed as a tool for reducing the computational cost of FE analysis of EM diffusion. It has been shown that POD is able to reduce the size of the matrices greatly and still maintain high accuracy. This is particularly important for large, 3-D computer simulations which can take days to finish. In FEM, the spatial domain is discretized into a high number of elements and consequently the fields are represented by a large number of basis functions. In the POD model, the spatial distributions are described by the first few and most relevant POD basis functions.

The matrices in the original FEM models are sparse, but the dimensions are high. The solutions must be found through lengthy iterative procedures. Although the matrices of the reduced models are dense, the dimensions are much lower. Overall, a desirable reduction of computational time is achieved elegantly.

The tests in this thesis were in 1-D and 2-D. The application to 3-D follows along exactly the same lines, but clearly there is a need to test POD TD-FEM on some large, realistic, 3-D problems to establish the accuracy and efficiency of the method in those cases.

TD-FEM is a powerful and versatile tool for analysis of a wide variety of other electromagnetic devices, including those where wave propagation rather than diffusion is the important process, e.g., antennas and microwave circuits [28]. It would be interesting to implement POD to reduce the matrices involved in those applications.

Therefore, much like the field of TD-FEM itself, the usage and future implications of POD remains very open. The balance between performance and cost in commercial design is increasingly important. So, possibilities abound for reduction methods such as POD.

In this thesis, the conventional POD was applied. A lot of work is going on in improving it. There are improved versions of POD such as Missing Point Estimation POD (MPE-POD) which has been proven to be much more efficient than conventional POD [29]. It is based upon the gappy POD method developed by Everson and Sirovich [30]. Some other developments of POD include the Group POD [31]. Some of these new variants might be effective when applied to TD-FEM. In another work [32], conventional POD and the combination with MPE were applied to a nonlinear heat conduction model. The reduced order model by POD-MPE was found to be 150 times faster than conventional time stepping, while the classic POD model was only about 10 times faster than the original one.

However, there are some limitations worth noting. POD might not be very useful when we want to simulate a short transient. Applying POD to situations like that would make it more complex for no purpose.

Different number of snapshots and eigenvectors produce different results. Fewer snapshots can help reduce computational cost (as it has been shown in this thesis) but also lead to lower accuracy. Use of a smaller set of eigenvectors can help reduce computations even further, but a too small a set will lead to high inaccuracy. Therefore, the question is to find the optimal number of snapshots and eigenvectors. For

successful commercial software, this decision has to be automated. If the user had to choose every time, it would make the whole process cumbersome. That is also an area for future research.

In this thesis work, POD has provided very satisfactory results. One can certainly assume that we will see successful implementations of POD in other areas of computational EM.

REFERENCES

1. Pearson, K. "On Lines and Planes of Closest Fit to Systems of Points in Space". Philosophical Magazine **2** (6): 559–572. , 1901.

2. Graham, M. D., Lane, S. L., & Luss, D. "Proper orthogonal decomposition: analysis of spatiotemporal temperature patterns". Journal of Physical Chemistry, 97(4), 889–894, 1993.

3. Berkooz, G., Holmes, P., & Lumley, J. L. "The proper orthogonal decomposition in the analysis of turbulent flows". Annual Review of Fluid Mechanics, 25, 539–575, 1993.

4. Pratt, K. W. "Digital image processing". New York: Wiley, 1991.

5. LeGresley, P. A. "Application of Proper Orthogonal Decomposition (POD) to Design Decomposition Methods". Ph.D. Dissertation, Stanford University, 2005.

6. Y.C. Liang et. al. "Proper Orthogonal Decomposition And Its Applications - Part II: Model Reduction for MEMS Dynamical Analysis". Journal of Sound and Vibration, Volume 256, Issue 3, 2002.

7. Preisendorfer. "Principal component analysis in meteorology and oceanography". R. In C. Mobley (Ed.), Amsterdam: Elsevier, 1988.

8. Pettit, C. L., & Beran, P. S. "Reduced-order modeling for flutter prediction". 41st AIAA/ASCE/AHS/ASC structural, structural dynamics and materials

conference, Atlanta, GA, 2000.

9. Wim A. Mulder, Marwan Wirianto, and Evert C. Slob. "Time-domain modeling of electromagnetic diffusion with a frequency-domain code". Geophysics, Vol. 73, No. 1, 2008.

10. David B. Davidson. "Computational Electromagnetics for RF and Microwave Engineering". Cambridge University Press, 2005.

11. A. Bondeson, T. Rylander & P' Ingelstorm. "Computational Electromagnetics". Springer, 2005.

12. Allen Taflove. "Computational electrodynamics : the finite-difference time-domain method". Boston : Artech House, 1995.

13. P. P. Silvester, R.L. Ferrari. "Finite elements for electrical engineers". Cambridge University Press, 1996.

14. Jianming Jin. "The Finite Element Method in Electromagnetics". Jon Wiley & Sons Inc., 2002.

15. G. Grandi, M. K. Kazimierczuk, A. Massarini, U. Reggiani, G. Sancineto."Model of Laminated Iron-Core Inductors for High Frequencies". IEEE Transactions on Magnetics, Vol. 40, No. 4, 2004.

16. S. Yamada and K. Bessho, "Harmonic field calculation by the combination of finite element analysis and harmonic balance method". IEEE Trans. Magn., Vol.

24, pp. 2588–2590, Nov. 1988.

17. R. A. Bialecki, A. J. Kassab and A. Fic. "Proper orthogonal decomposition and modal analysis for acceleration of transient FEM thermal analysis". Int. J. Numer. Meth. Engng , 62:774–797, 2005.

18. Takahashi, Y. et. al.. "Convergence Acceleration of Time-Periodic Electromagnetic Field Analysis by the Singularity Decomposition-Explicit Error Correction Method". IEEE Transactions on Magnetics, Vol. 46, No. 8, August 2010.

19. P. P. Silvester. "Modern Electromagnetic Fields". Prentice-Hall, Inc., 1968.

20. Isaak Mayergoyz. "Nonlinear Diffusion of Electromagnetic Fields". Academic Press, 1998.

21. MagNet 7.1.2, 2010, Infolytica Corporation, Montreal, Canada. *http://www.infolytica.com/*

22. H. Hotelling. "Analysis of a complex of statistical variables into principal components". The Journal of Educational Psychology, 1933.

23. K. Karhunen. "Zur spektraltheorie stochastischer prozesse". Ann. Acad. Sci. Fennicae, Ser.A1, 34, 1946.

24. M. Loeve. "Funcions aleatoire de second ordre". Comptes Rendus Acad. Sci. Paris, 220, 1945.

25. Sirovich, L. "Turbulence and the dynamics of coherent structures". Quarterly of Applied Mathematics, 5, 561–590. 1987.

26. *http://www.mathworks.com*

27. G. H. Golub, C. F. Van Loan, "Matrix Computations". Johns Hopkins, 1983.

28. J. M. Jin and D. J. Riley, "Finite Element Analysis of Antennas and Arrays". Hoboken, NJ: Wiley, 2009.

29. Patricia Astrid, Siep Weiland, Karen Willcox, Ton Backx. "Missing point estimation in models described by proper orthogonal decomposition". 43rd IEEE Conference on Decision and Control, Atlantis, Paradise Island, Bahamas, December 14-17, 2004.

30. R. Everson and L. Sirovich. "The Karhunen-Loeve Procedure for Gappy Data". J.Opt.Soc.Am., 12: 1657-1664, 1995.

31. Benjamin T. Dickinson and John R. Singler. "Nonlinear Model Reduction Using Group Proper Orthogonal Decomposition". International Journal of Numerical Analysis and Modeling, 2010.

32. Patricia Astrid. "Reduction of Process Simulation Models: a proper orthogonal decomposition approach". Ph.D. Dissertation, Technische Universiteit Eindhoven, 2004.